Generalized Invariance Principles for Stochastic Dynamical Systems and Their Applications

Shijie Zhou, Wei Lin *Senior Member, IEEE*, Xuerong Mao, and Jianhong Wu

***Abstract*—Investigating long-term behaviors of stochastic dynamical systems often requires to establish criteria that are able to describe delicate dynamics of the considered systems. In this article, we develop generalized invariance principles for continuous-time stochastic dynamical systems. Particularly, in a sense of probability one and by the developed semimartingale convergence theorem, we not only establish a local invariance principle, but also provide a generalized global invariance principle that allows the sign of the diffusion operator to be positive in some bounded region. We further provide an estimation for the time when a trajectory, initiating outside a particular bounded set, eventually enters it. Finally, we use several representative examples, including stochastic oscillating dynamics, to illustrate the practical usefulness of our analytical criteria in deciphering the stabilization or/and the synchronization dynamics of stochastic systems.**

***Index Terms*—Invariance principle; local and global invariance; stochastic dynamical systems; time estimation**

I. Introduction

Long-term behaviors of complex systems have received wide attention [63], [64]. Various types of theories have been developed systematically, including Lyapunov stability theories and invariance principles [2], [3], [13], [39], [56], [57], [61], center manifold and bifurcation theories [26], [27], [40], [41], [55], [60], and chaos theories. The classical invariance principle [1], which first originated from the Lyapunov second methods [39], has been performed and extended from finitely to infinitely dimensional spaces [4], [5], from autonomous to non-autonomous dynamical systems [6], [7], [14], [37], [38], from time-homogeneous to switching systems [8], [9], [45], [50], [54], and from asymptotic synchronization and transient chaos [24], [25], [53].

On the other hand, noise, which is unavoidable in real systems, always makes it difficult but worthwhile to investigate complex dynamics because it could bring about not only uncertainty and disorder but also counter-initiative phenomena. Several noise-induced phenomena have been studied in the literature, such as stochastic resonance [10], stochastic stabilization or/and synchronization [11], [20], [21], [25], [46], random-temporal-structure-induced emergence [12], [15]–[18], [48]–[51]. Also developed was the stochastic version of LaSalle's invariance principle [31]–[34], [45]–[47], [52], [53], which describes the asymptotic stability of a stochastic dynamical system by using a Lyapunov function or functional.

When applying such stochastic LaSalle's invariance principles, one, according to the principles in the classical textbook, usually needs to construct a Lyapunov function whose diffusion operator (denoted by $\mathscr{L}V$; see below for the definition) is assumed to be at least negative semidefinite. However, constructing such Lyapunov function is always difficult. Even in the more generalized version of the theory [28], [35], [36], the efficient criteria are still hard to satisfy because multiple Lyapunov functions are needed. In addition, most of these theories are used to study stochastic asymptotic stability, which greatly limits the feasible range. Therefore, a generalized version of invariance principle which allows the sign of the diffusion operator to be positive is highly required.

In this article, we are to establish invariance principles for stochastic autonomous differential equations. Significantly, in a sense of probability one, we not only establish a local invariance principle, but also provide a generalized global invariance principle which allows the sign of the diffusion operator to be positive in a bounded region. In addition, we depict global dynamics by estimating the time for a trajectory to enter or stay in a particular set. Finally, we use several representative examples, including studying the stochastic synchronized neural dynamics, to demonstrate the practical usefulness of our theories.

The rest of this article is organized as follows. In Section II, we describe model formulation and provide some extended mathematical conditions. In Section III, we present our main results for ensuring both local and global invariance. In Section IV, we give the detailed proofs of the main theorems. Finally in Section V, we provide several illustrative examples, including some biological stochastic models, for demonstrating the broad applicability of our main results.

II. Model Description and Useful Conditions

To begin with, we consider a p-dimensional continuous-time stochastic dynamical system

$$\mathrm{d}\boldsymbol{x}_t = \boldsymbol{f}(\boldsymbol{x}_t)\mathrm{d}t + \boldsymbol{g}(\boldsymbol{x}_t)\mathrm{d}\boldsymbol{B}_t, \tag{1}$$

with the initial state $\boldsymbol{x}(0) = \boldsymbol{x}_0 \in \mathbb{R}^p$. Here, $\boldsymbol{f} : \mathbb{R}^p \to \mathbb{R}^p$ and $\boldsymbol{g} : \mathbb{R}^p \to \mathbb{R}^{p\times m}$ are both continuous functions and $\boldsymbol{B}_t = [B_1(t), B_2(t), \cdots, B_m(t)]^\top$ is a standard m-dimensional Brownian motion. Furthermore, we denote by $(\Omega, \mathscr{F}, \{\mathscr{F}_t\}_{t\geq 0}, \mathbb{P})$

Shijie Zhou is with the Department of Mathematics and Statistics, York University, Toronto M3J3R6, Canada (e-mail: sjzhou14@fudan.edu.cn)

Wei Lin is with the School of Mathematical Sciences, Centre for Systems Computational Biology, and Institute of Science and Technology for Brain-Inspired Intelligence, Fudan University, Shanghai 200433, China and with the Shanghai Key Laboratory of Contemporary Applied Mathematics and Key Laboratory of Mathematics for Nonlinear Sciences (Fudan University), Ministry of Education, China (e-mail: wlin@fudan.edu.cn)

Xuerong Mao is with the Department of Mathematics and Statistics, University of Strathclyde, Glasgow G11XH, UK

Jianhong Wu is with the Department of Mathematics and Statistics, York University, Toronto M3J3R6, Canada

W. Lin, to whom correspondence should be addressed. Tel. +86-21-55665141. Fax. +86-21-65646073.

the complete probability space with a filtration $\mathscr{F}_t$ satisfying the usual condition (i.e., it is increasing and right continuous while $\mathscr{F}_0$ contains all $\mathbb{P}$-null sets) where the m-dimensional Brownian motion $\boldsymbol{B}_t$ in system (1) is well defined.

According to the classical theory of stochastic differential equations [29], we need locally Lipschitizian conditions for the vector field $\boldsymbol{f}$ and $\boldsymbol{g}$ in the following to ensure the uniqueness and existence of the solution of system (1).

Condition 2.1: (Locally Lipschitzian condition) For any given positive number n, there exists a positive number K_n such that

$$\|\boldsymbol{f}(\boldsymbol{x})-\boldsymbol{f}(\boldsymbol{y})\| \le K_n\|\boldsymbol{x}-\boldsymbol{y}\|, \quad \|\boldsymbol{g}(\boldsymbol{x})-\boldsymbol{g}(\boldsymbol{y})\| \le K_n\|\boldsymbol{x}-\boldsymbol{y}\|,$$

for any $\boldsymbol{x},\boldsymbol{y} \in \mathbb{R}^p$ with $\|\boldsymbol{x}\| \le n$ and $\|\boldsymbol{y}\| \le n$. Here, $\|\cdot\|$ represents any appropriate norm in $\mathbb{R}^n$ or $\mathbb{R}^{n\times m}$.

Akin to the traditional Lyapnouv approach in the ordinary differential equation, we use a continuously twice differentiable function $V : \mathbb{R}^p \to \mathbb{R}$ which satisfies particular conditions to study the dynamics of system (1). One of the typical constraints on function V is presented as follows.

Condition 2.2: Function V satisfies that $\lim_{\|\boldsymbol{x}\|\to+\infty} V(\boldsymbol{x}) = +\infty$ and $V(\boldsymbol{x}) \ge 0$ for all $\boldsymbol{x} \in \mathbb{R}^p$.

In the theory of stochastic version of invariance principle, the Itô formula plays a vital role. The differential form of Itô's formula [29] on V is as such:

$$\mathrm{d}V(\boldsymbol{x}_t) = \mathscr{L}V(\boldsymbol{x}_t)\mathrm{d}t + \mathscr{D}V(\boldsymbol{x}_t)\mathrm{d}\boldsymbol{B}_t, \tag{2}$$

where two operators $\mathscr{L}$ and $\mathscr{D}$ acting on continuously twice differentiable functions are denoted, respectively, by

$$\mathscr{L}V(\boldsymbol{x}) \triangleq V_{\boldsymbol{x}}(\boldsymbol{x})\boldsymbol{f}(\boldsymbol{x}) + \frac{1}{2}\mathrm{trace}\Big[\boldsymbol{g}^\top(\boldsymbol{x})V_{\boldsymbol{x}\boldsymbol{x}}(\boldsymbol{x})\boldsymbol{g}(\boldsymbol{x})\Big],$$

and $\mathscr{D}V(\boldsymbol{x}) \triangleq V_{\boldsymbol{x}}(\boldsymbol{x})\boldsymbol{g}(\boldsymbol{x})$. Here, the derivatives

$$V_{\boldsymbol{x}}(\boldsymbol{x}) = \left[\frac{\partial V(\boldsymbol{x})}{\partial x_1}, \frac{\partial V(\boldsymbol{x})}{\partial x_2}, \cdots, \frac{\partial V(\boldsymbol{x})}{\partial x_p}\right],\ V_{\boldsymbol{x}\boldsymbol{x}}(\boldsymbol{x}) = \left[\frac{\partial^2 V(\boldsymbol{x})}{\partial x_i \partial x_j}\right]_{p\times p}$$

stand, respectively, for the gradient vector and the Jacobian matrix of $V(\boldsymbol{x})$.

Denote a series of increasing open sets by

$$\mathscr{M}_r \triangleq \{\boldsymbol{x} \in \mathbb{R}^p \mid \mathscr{L}V(\boldsymbol{x}) > -r\}$$

for $r \in \mathbb{R}$, and denote an increasing left continuous function by $p(r) \triangleq \sup_{\boldsymbol{x}\in\mathscr{M}_r} V(\boldsymbol{x})$, which can be used to characterize these sets. The following condition depicts the properties of the set $\mathscr{M}_0$, one of the most important sets among them.

Condition 2.3: $\mathscr{M}_0$ is a bounded and nonempty set, which indicates $p(0) < +\infty$.

III. Main Results

In this section, we establish several generalized versions of invariance principle.

First, we articulate a version which guarantees that some particular set is invariant under the evolution of system (1) in the sense of probability one .

Theorem 3.1: (Local invariance principle) Assume that, for a given twice differentiable function $V : \mathbb{R}^p \to \mathbb{R}$, the set $\{\boldsymbol{x} \in \mathbb{R}^p \mid V(\boldsymbol{x}) = C\}$, if it is a $(p-1)$-dimensional manifold, can divide $\mathbb{R}^p$ into two parts: $\big\{\boldsymbol{x} \in \mathbb{R}^p \mid V(\boldsymbol{x}) < C\big\}$ and $\big\{\boldsymbol{x} \in \mathbb{R}^p \mid V(\boldsymbol{x}) > C\big\}$. If there exist three numbers $\delta, k_1, k_2 > 0$ such that

$$\mathscr{L}V(\boldsymbol{x}) \le k_1[C - V(\boldsymbol{x})] \quad (\text{resp., } \mathscr{L}V(\boldsymbol{x}) \ge -k_1[V(\boldsymbol{x}) - C])$$

and $\big\|\mathscr{D}V(\boldsymbol{x})\big\| \le k_2\big|C - V(\boldsymbol{x})\big|$ for

$$\big\{\boldsymbol{x} \in \mathbb{R}^p \mid C - \delta \le V(\boldsymbol{x}) \le C\big\} \qquad (\text{resp., } \big\{\boldsymbol{x} \in \mathbb{R}^p \mid C + \delta \ge V(\boldsymbol{x}) \ge C\big\}).$$

Then, for any initial state $\boldsymbol{x}_0$ which satisfies $V(\boldsymbol{x}_0) < C$ (resp., $V(\boldsymbol{x}_0) > C$), the trajectory of system (1) does not leave the set $\big\{\boldsymbol{x} \in \mathbb{R}^p \mid V(\boldsymbol{x}) < C\big\}$ (resp., $\big\{\boldsymbol{x} \in \mathbb{R}^p \mid V(\boldsymbol{x}) > C\big\}$) in a finite-time duration almost surely.

Remark 3.2: The condition in Theorem 3.1 indicates that, on the manifold $\{\boldsymbol{x} \in \mathbb{R}^p \mid V(\boldsymbol{x}) = C\}$ of $(p-1)$-dimension, we have $\mathscr{L}V(\boldsymbol{x}) \le 0$ (or $\mathscr{L}V(\boldsymbol{x}) \ge 0$) and $\mathscr{D}V(\boldsymbol{x}) = \boldsymbol{0}$. Intuitively speaking, it indicates that, if on the boundary of a specified "ball", the diffusive term, $\mathscr{L}V(\boldsymbol{x})$, makes the trajectory enter (or leave) the "ball" and the noise is tangent to the surface, then the trajectory never leaves (or enters) the "ball".

Next, we need to validate a global invariance principle for system (1). We first present a result on the global existence and uniqueness of the solution for system (1), which can be seen as a foot-stone for any deeper discussions.

Theorem 3.3: Assume Conditions 2.1-2.3 are all fulfilled. Then, for any initial state $\boldsymbol{x}_0 \in \mathbb{R}^p$, the trajectory $\boldsymbol{x}_t$ in system (1) is existent on the entire interval $[0, +\infty)$ almost surely, so that it does not explode in any finite-time duration almost surely.

The following theorem depicts the trajectory of system (1) in different types.

Theorem 3.4: Denote by

$$\Omega_1 \triangleq \left\{\lim_{t\to+\infty} \mathrm{dist}(\boldsymbol{x}_t, \mathscr{A}) = 0 \text{ and } \lim_{t\to+\infty} V(\boldsymbol{x}_t) \text{ exists finitely}\right\},$$

and by

$$\Omega_2 \triangleq \Big\{\boldsymbol{x}_t \text{ travels in between } \mathscr{M}_0 \text{ and } \mathscr{N} \text{ for infinite number of times}\Big\},$$

where

$$\mathscr{A} = \Big\{\boldsymbol{x} \in \mathbb{R}^p \mid \mathscr{L}V(\boldsymbol{x}) = 0,\ \mathscr{D}V(\boldsymbol{x}) = \boldsymbol{0}\Big\} \tag{3}$$

and $\mathscr{N} = \big\{\boldsymbol{x} \in \mathbb{R}^p \mid \mathscr{L}V(\boldsymbol{x}) < 0\big\}$. Assume that Conditions 2.1-2.3 are all fulfilled. Then, $\Omega = \Omega_1 \cup \Omega_2$, a.s.. Here and throughout, "a.s." represents an abbreviation of "almost surely".

Remark 3.5: Theorem 3.4 describes how the trajectory of system (1) evolves in the phase space in the presence of stochastic perturbations. However, in most cases, the probability $\mathbb{P}(\Omega_1) \ll 1$ or even it is zero. Thus, we need a more delicate description for the trajectory in Ω_2. Next theorem renders it possible to estimate the time when an orbit, initiating outside a particular bounded set, finally enters it.

Theorem 3.6: Assume that Conditions 2.1-2.3 are all valid and that, for some positive r, $p(r) < +\infty$. If ν is a stopping time which satisfies $\mathscr{L}V(\boldsymbol{x}_\nu) < -r$ in the set $\{\nu < +\infty\}$ and $\mathbb{E}[V(\boldsymbol{x}_\nu); \nu < +\infty] < +\infty$. Denote a stopping time by $\mu \triangleq \inf\left\{t > \nu \;\middle|\; V(\boldsymbol{x}_t) \le p(r)\right\}$. Then, we have

$$\mathbb{E}[\mu - \nu; \nu < +\infty] \le \frac{1}{r}\mathbb{E}[V(\boldsymbol{x}_\nu); \nu < +\infty] - \frac{p(r)}{r}\mathbb{P}[\nu < +\infty].$$

Remark 3.7: Theorem 3.6 gives a rough estimation for the time that a trajectory needs to approach particular sets. In fact, when $p(r)$ is smooth, a more precise estimation can be given.

Theorem 3.8: If $V(\boldsymbol{x}_0) > p(R)$ for some $R > 0$ and $\mathbb{E}V(\boldsymbol{x}_0) < +\infty$. Denote a stopping time by

$$\mu \triangleq \inf\left\{t > 0 \;\middle|\; V(\boldsymbol{x}_t) \le p(r)\right\}.$$

If $p(r)$ is differentiable, then we have

$$\mathbb{E}[\mu] \le \frac{\mathbb{E}V(\boldsymbol{x}_0) - p(R)}{R} + \int_r^R \frac{p'(s)}{s}\mathrm{d}s. \tag{4}$$

Theorem 3.9: Denote an index by $f_r(t) = \int_0^t \mathbf{1}_{\boldsymbol{x}_s \in \mathscr{M}_r}\mathrm{d}s$, where $\mathbf{1}_{\mathscr{S}}$ is the standard indicator function with respect to a given set $\mathscr{S}$ and $r > 0$. Assume that both Conditions 2.1 & 2.3 are valid. Then, we have

$$\left\{\liminf_{t\to+\infty} \frac{f_r(t)}{t} \ge \frac{r}{r+B}\right\} \subseteq \Omega_3 \triangleq \left\{\sup_{t>0}\|\boldsymbol{x}_t\| < +\infty\right\} \text{ a.s.}, \tag{5}$$

where $B \triangleq \sup_{\boldsymbol{x}\in\mathbb{R}^p} \mathscr{L}V(\boldsymbol{x}) < +\infty$.

Remark 3.10: Theorem 3.9 shows that the trajectory stays in a particular set for a large amount of time. Although we cannot confirm the boundedness of the solution of system (1) analytically in many cases, the time estimation presented in (5) is still valid in most cases. Such validity will be shown in the latter section using a number of representative examples.

IV. Proofs of Main Theorems

Here, we include the detailed proofs for all the main theorems established in Section III.

Proof of Theorem 3.1. We only need to prove the situation in which $V(\boldsymbol{x}_0) < C$. The proof for the other side case is similar. Denote by χ the time when trajectory leaves the set $\left\{\boldsymbol{x} \in \mathbb{R}^p \;\middle|\; V(\boldsymbol{x}) < C\right\}$. Denote by an increasing sequence of stopping times as follows:

$$\begin{aligned}
\psi_1 &\triangleq \inf\{t \,|\, V(\boldsymbol{x}_t) \ge C - \frac{\delta}{2}\},\\
\psi_2 &\triangleq \inf\{t \ge \psi_1 \,|\, V(\boldsymbol{x}_t) < C - \delta\}, \cdots\\
\psi_{2n+1} &\triangleq \inf\{t \ge \psi_{2n} \,|\, V(\boldsymbol{x}_t) \ge C - \frac{\delta}{2}\},\\
\psi_{2n+2} &\triangleq \inf\{t \ge \psi_{2n+1} \,|\, V(\boldsymbol{x}_t) < C - \delta\}, \cdots
\end{aligned}$$

where $\psi_0 = 0$ and $\inf\emptyset = +\infty$.

First, we need to validate that $\lim_{n\to+\infty}\psi_n = +\infty$. If this is not the case, suppose that $\lim_{n\to+\infty}\psi_n = M < +\infty$. Due to the continuity of $\boldsymbol{x}_t$, we obtain that

$$C - \frac{\delta}{2} = \lim_{n\to+\infty} V(\boldsymbol{x}_{\psi_{2n+1}}) = V(M) = \lim_{n\to+\infty} V(\boldsymbol{x}_{\psi_{2n+2}}) = C - \delta,$$

which is a contradiction.

If $\mathbb{P}[\chi < +\infty] > 0$, then there exists an integral number n such that

$$\mathbb{P}[\psi_{2n+1} < \chi < \psi_{2n+2}; \psi_{2n+1} < +\infty] > 0.$$

Denote by $\chi_\epsilon \triangleq \inf\left\{t \ge \psi_{2n+1} \;\middle|\; V(\boldsymbol{x}_t) \ge C - \epsilon\right\}$ for sufficiently small ϵ. Thus, $\lim_{\epsilon\to0+}\chi_\epsilon = \chi$. Applying Itô's formula to $\log[C - V(\boldsymbol{x}_t)]$ on the time interval $[\psi_{2n+1}, \psi_{2n+2} \wedge (\psi_{2n+1} + t) \wedge \chi_\epsilon]$ yields:

$$\begin{aligned}
&\log\left[C - V(\boldsymbol{x}_{\psi_{2n+2}\wedge(\psi_{2n+1}+t)\wedge\chi_\epsilon})\right] = \log\left[C - V(\boldsymbol{x}_{\psi_{2n+1}})\right]\\
&\quad + \int_{\psi_{2n+1}}^{\psi_{2n+2}\wedge(\psi_{2n+1}+t)\wedge\chi_\epsilon} \left\{\frac{\mathscr{L}V(\boldsymbol{x}_s)}{V(\boldsymbol{x}_s) - C} - \frac{1}{2}\frac{\left\|\mathscr{D}V(\boldsymbol{x}_s)\right\|^2}{[V(\boldsymbol{x}_s) - C]^2}\right\}\mathrm{d}s\\
&\quad + \int_{\psi_{2n+1}}^{\psi_{2n+2}\wedge(\psi_{2n+1}+t)\wedge\chi_\epsilon} \frac{\mathscr{D}V(\boldsymbol{x}_s)}{V(\boldsymbol{x}_s) - C}\mathrm{d}\boldsymbol{B}_s.
\end{aligned}$$

Multiplying both sides by $\mathbf{1}_{\psi_{2n+1}<+\infty}$ and then taking expectation on both sides give

$$\begin{aligned}
&\log\epsilon \cdot \mathbb{P}[\psi_{2n+1} < \chi_\epsilon < \psi_{2n+2} \wedge (\psi_{2n+1} + t); \psi_{2n+1} < +\infty]\\
&\quad + \log\delta \cdot \Big\{\mathbb{P}(\psi_{2n+1} < +\infty)\\
&\quad - \mathbb{P}[\psi_{2n+1} < \chi_\epsilon < \psi_{2n+2} \wedge (\psi_{2n+1} + t); \psi_{2n+1} < +\infty]\Big\}\\
&\ge \mathbb{E}\Big[\log\left[C - V(\boldsymbol{x}_{\psi_{2n+1}})\right]; \psi_{2n+1} < +\infty\Big]\\
&- \left(k_1 + \frac{k_2^2}{2}\right)t \cdot \mathbb{P}\left[\psi_{2n+1} < +\infty\right]\\
&\ge \log\left[\frac{\delta}{2}\right] \cdot \mathbb{P}\left[\psi_{2n+1} < +\infty\right] - \left(k_1 + \frac{k_2^2}{2}\right)t \cdot \mathbb{P}\left[\psi_{2n+1} < +\infty\right].
\end{aligned}$$

Letting $\epsilon \to 0+$ and $t \to +\infty$ in the above inequality enables us to get

$$\mathbb{P}[\psi_{2n+1} < \chi < \psi_{2n+2}; \psi_{2n+1} < +\infty] = 0,$$

which is a contradiction. ■

Proof of Theorem 3.3. We are to prove that the trajectory of system (1) does not diverge in a finite time duration. Condition 2.3 implies that there exists a positive number C such that $\mathscr{L}V(\boldsymbol{x}) \le C$ for any $\boldsymbol{x} \in \mathbb{R}^p$. Denote by $\sigma_r \triangleq \inf\{t \ge 0 | V(\boldsymbol{x}_t) \ge r\}$, and denote the explosion time by $\sigma_\infty \triangleq \lim_{r\to+\infty}\sigma_r$.

The integral form of (2) on the interval $[0, \sigma_r \wedge t]$ yields:

$$V(\boldsymbol{x}_{\sigma_r\wedge t}) = V(\boldsymbol{x}_0) + \int_0^{\sigma_r\wedge t} \mathscr{L}V(\boldsymbol{x}_s)\mathrm{d}s + \int_0^{\sigma_r\wedge t} \mathscr{D}V(\boldsymbol{x}_s)\mathrm{d}\boldsymbol{B}_t. \tag{6}$$

By taking the expectation on both sides of Eq. (6), we obtain $\mathbb{E}[V(\boldsymbol{x}_{\sigma_r\wedge t})] \le \mathbb{E}[V(\boldsymbol{x}_0)] + Ct$. A further estimation yields

$$r\mathbb{P}[\sigma_r \le t] \le \mathbb{E}[V(\boldsymbol{x}_{\sigma_r\wedge t})] \le \mathbb{E}[V(\boldsymbol{x}_0)] + Ct,$$

which further indicates that

$$\mathbb{P}[\sigma_\infty \le t] = \lim_{r\to+\infty}\mathbb{P}[\sigma_r \le t] = 0.$$

Letting $t \to +\infty$ here enables us to get $\mathbb{P}[\sigma_\infty < +\infty] = 0$. This completes the proof. ■

Proof of Theorem 3.4. Denote two increasing sequences of stopping times as: $\gamma_n^1 \triangleq \inf\{t \ge n \mid \mathscr{L}V(\boldsymbol{x}_t) > 0\}$ and $\gamma_n^2 \triangleq \inf\{t \ge n \mid \mathscr{L}V(\boldsymbol{x}_t) < 0\}$. Obviously, $\lim_{n\to+\infty}\gamma_n^i =$

$+\infty$, $i=1,2$. Hence, Ω can be decomposed into three disjoint measurable sets, i.e., $\Omega=\Gamma^1\cup\Gamma^2\cup\Gamma^3$, in which

$$\Gamma^i \triangleq \Big\{\text{There exists a positive integral number } n \text{ such that } \gamma_n^i=+\infty\Big\},\ i=1,2,$$

and

$$\Gamma^3 \triangleq \Big\{\text{For all positive integral numbers } n,\ \gamma_n^1<+\infty \text{ and } \gamma_n^2<+\infty\Big\}.$$

Obviously, Γ^3 is equal to the set Ω_2 as defined above.

The integral form of Eq. (2) can be written as

$$V(\boldsymbol{x}_t)=V(\boldsymbol{x}_0)+A_t^1-A_t^2+M_t, \tag{7}$$

where

$$A_t^1=\int_0^t \mathscr{L}V(\boldsymbol{x}_s)\mathbf{1}_{\mathscr{L}V(\boldsymbol{x}_s)>0}\mathrm{d}s,$$

$$A_t^2=-\int_0^t \mathscr{L}V(\boldsymbol{x}_s)\mathbf{1}_{\mathscr{L}V(\boldsymbol{x}_s)<0}\mathrm{d}s,\ \text{and}\ M_t=\int_0^t \mathscr{D}V(\boldsymbol{x}_s)\mathrm{d}\boldsymbol{B}_s.$$

For any event $\omega\in\Gamma^1$, there exists a positive number $T(\omega)$, such that $\mathscr{L}V(\boldsymbol{x}_t)\le 0$ for $t\ge T(\omega)$, which further indicates that $\lim_{t\to+\infty}A_t^1<+\infty$.

With the validity of Condition 2.2, we have $V(\boldsymbol{x}_t)\ge 0$. According to Lemma 7.1, we conclude that

$$\Gamma^1\subseteq\Big\{\lim_{t\to+\infty}A_t^2<+\infty\Big\}\cap\Big\{\lim_{t\to+\infty}V(\boldsymbol{x}_t)\text{ exists finitely}\Big\}\text{ a.s..}$$

Furthermore, $\lim_{t\to+\infty}A_t^2<+\infty$, together with $\mathscr{L}V(\boldsymbol{x}_t)\le 0$ for $t>T$, implies that $\int_0^{+\infty}|\mathscr{L}V(\boldsymbol{x}_s)|\mathrm{d}s<+\infty$ for almost every event $\omega\in\Gamma^1$.

Another conclusion that $\lim_{t\to+\infty}V(\boldsymbol{x}_t)$ exists finitely, with Condition 2.2, gives that $\sup_{t>0}\|\boldsymbol{x}_t\|<+\infty$ almost surely. Applying Lemma 7.2 results in a conclusion that $\lim_{t\to+\infty}\mathscr{L}V(\boldsymbol{x}_t)=0$ almost surely in Γ^1.

At last, we need to validate that $\lim_{t\to+\infty}\mathscr{D}V(\boldsymbol{x}_t)=\mathbf{0}$. For this, we consider $Q(x)=-\mathrm{e}^{-x}$. A direct calculation leads to

$$\mathscr{L}Q[V(\boldsymbol{x}_t)]=\mathrm{e}^{-V(\boldsymbol{x}_t)}\left[\mathscr{L}V(\boldsymbol{x}_t)-\frac{1}{2}\left\|\mathscr{D}V(\boldsymbol{x}_t)\right\|^2\right],$$

Thus, $\mathscr{L}Q[V(\boldsymbol{x}_t)]\le 0$ for $t>T(\omega)$. Since we have derived that

$$\Gamma^1\subseteq\Big\{\lim_{t\to+\infty}Q[V(\boldsymbol{x}_t)]\text{exists finitely}\Big\}\text{ a.s.,}$$

an application of Lemma 7.1 to the semimartingale $Q[V(\boldsymbol{x}_t)]$ yields a convergence of the integral, i.e.,

$$\int_0^{+\infty}\left|\mathscr{L}Q[V(\boldsymbol{x}_s)]\right|\mathrm{d}s<+\infty\text{ a.s..}$$

Using Lemma 7.2 again results in a limit, i.e., $\lim_{t\to+\infty}\mathscr{L}Q[V(\boldsymbol{x}_t)]=0$, which further suggests, in Γ^1, $\lim_{t\to+\infty}\mathscr{D}V(\boldsymbol{x}_t)=\mathbf{0}$ almost surely.

Finally, we need to prove that $\lim_{t\to+\infty}\mathrm{dist}(\boldsymbol{x}_t,\mathscr{A})=0$ in Γ^1. If this is not the case, we can find a number $h>0$ and a sequence $\{t_k\}$ such that $\lim_{k\to+\infty}t_k=+\infty$ and $\mathrm{dist}(\boldsymbol{x}_{t_k},\mathscr{A})>h$. Since $\boldsymbol{x}_{t_k}$ is bounded, it is reasonable to suppose that $\lim_{k\to+\infty}\boldsymbol{x}_{t_k}=\boldsymbol{x}^*$ a.s.. This convergence indicates that $\mathrm{dist}(\boldsymbol{x}^*,\mathscr{A})\ge h$, $\mathscr{L}V(\boldsymbol{x}^*)=0$, and $\mathscr{D}V(\boldsymbol{x}^*)=\mathbf{0}$. From the definition of $\mathscr{A}$, we get a contradiction. This completes the proof of $\Gamma^1\subseteq\Omega^1$ a.s..

Similarly, for every event $\omega\in\Gamma^2$, we consider the decomposition of the semimartingale as follows:

$$-V(\boldsymbol{x}_t)=-V(\boldsymbol{x}_0)+A_t^2-A_t^1-M_t, \tag{8}$$

where A_t^1, A_t^2 and M_t are the same as those in (7). There also exists $T(\omega)>0$ such that $\mathscr{L}V(\boldsymbol{x}_t)\ge 0$ for $t>T(\omega)$, which indicates that $\sup_{t>T(\omega)}V(\boldsymbol{x}_t)\le p(0)$ a.s.. This suggests that the increasing process $\lim_{t\to+\infty}A_t^2<+\infty$ a.s. and $\inf_{t>0}-V(\boldsymbol{x}_t)>-\infty$ a.s.. Similarly, an application of Lemmas 7.1 and 7.2 again yields $\Gamma^2\subseteq\Omega^1$ a.s. This completes the whole proof of the theorem. ■

Proof of Theorem 3.6. Applying Itô's formula to the considered system on the time interval $[\nu,(\nu+t)\wedge\mu]$ yields that

$$\begin{aligned}&V(\boldsymbol{x}_{(\nu+t)\wedge\mu})\\&=V(\boldsymbol{x}_\nu)+\int_\nu^{(\nu+t)\wedge\mu}\mathscr{L}V(\boldsymbol{x}_s)\mathrm{d}s+\int_\nu^{(\nu+t)\wedge\mu}\mathscr{D}V(\boldsymbol{x}_s)\mathrm{d}\boldsymbol{B}_s.\end{aligned} \tag{9}$$

By taking the expectation on both sides, we get an estimation as:

$$\begin{aligned}&\mathbb{E}[V(\boldsymbol{x}_{(\nu+t)\wedge\mu});\nu<+\infty]\\&\le\mathbb{E}[V(\boldsymbol{x}_\nu);\nu<+\infty]-r\mathbb{E}[(\nu+t)\wedge\mu-\nu;\nu<+\infty].\end{aligned}$$

Since $V(\boldsymbol{x}_{(\nu+t)\wedge\mu})\ge p(r)$, we have that

$$\mathbb{E}[(\nu+t)\wedge\mu-\nu;\nu<+\infty]\le\frac{\mathbb{E}[V(\boldsymbol{x}_\nu);\nu<+\infty]-p(r)\mathbb{P}[\nu<+\infty]}{r}.$$

Therefore, letting $t\to+\infty$ completes the proof. ■

Remark 4.1: A direct corollary of this theorem is that if $\mathbb{E}[V(\boldsymbol{x}_\nu);\nu<+\infty]<+\infty$, $\mu<+\infty$ a.s. in the set $\{\nu<+\infty\}$.

Proof of Theorem 3.8. Define stopping times by

$$\mu_s\triangleq\inf\Big\{t>\nu\ \Big|\ V(\boldsymbol{x}_t)\le p(s)\Big\}$$

for $s\le R$. We select $r=r_0<r_1<r_2<\cdots<r_n=R$. Thus, we have

$$\mathbb{E}[\mu_{r_n}]\le\frac{\mathbb{E}V(\boldsymbol{x}_0)-p(r_n)}{r_n},\ \mathbb{E}[\mu_{r_{n-1}}-\mu_{r_n}]\le\frac{p(r_n)-p(r_{n-1})}{r_{n-1}},\cdots$$

$$\mathbb{E}[\mu_{r_{k-1}}-\mu_{r_k}]\le\frac{p(r_k)-p(r_{k-1})}{r_{k-1}},\ \mathbb{E}[\mu_{r_0}-\mu_{r_1}]\le\frac{p(r_1)-p(r_0)}{r_0}.$$

The summation of these inequalities yields the following estimation:

$$\mathbb{E}[\mu]\le\frac{\mathbb{E}V(\boldsymbol{x}_0)-p(R)}{R}+\sum_{k=1}^n\frac{p(r_k)-p(r_{k-1})}{r_{k-1}}.$$

When $\max_{1\le k\le n}[r_k-r_{k-1}]\to 0$, the summation of the right-hand side of the inequality converges to a Lebesgue Stieltjes Integral. This thus leads to an estimation as

$$\mathbb{E}[\mu]\le\frac{\mathbb{E}V(\boldsymbol{x}_0)-p(R)}{R}+\int_r^R\frac{1}{s}\mathrm{d}p(s).$$

As $p(r)$ is differentiable, it can written as

$$\mathbb{E}[\mu]\le\frac{\mathbb{E}V(\boldsymbol{x}_0)-p(R)}{R}+\int_r^R\frac{p'(s)}{s}\mathrm{d}s. \tag{10}$$

This completes the proof. ■

Proof of Theorem 3.9. The integral form of system (2) yields that

$$V(\boldsymbol{x}_t) = V(\boldsymbol{x}_0) + \int_0^t \mathscr{L}V(\boldsymbol{x}_s)\mathrm{d}s + \int_0^t \mathscr{D}V(\boldsymbol{x}_s)\mathrm{d}\boldsymbol{B}_s,$$

which can be rewritten as

$$\begin{aligned}&\frac{V(\boldsymbol{x}_t) - V(\boldsymbol{x}_0)}{t} - \frac{\int_0^t \mathscr{D}V(\boldsymbol{x}_s)\mathrm{d}\boldsymbol{B}_s}{t}\\ &= \frac{\int_0^t \mathscr{L}V(\boldsymbol{x}_s)\mathbf{1}_{\boldsymbol{x}_s\in\mathscr{M}_r}\mathrm{d}s}{t} + \frac{\int_0^t \mathscr{L}V(\boldsymbol{x}_s)\mathbf{1}_{\boldsymbol{x}_s\notin\mathscr{M}_r}\mathrm{d}s}{t}.\end{aligned} \tag{11}$$

Since, for $\boldsymbol{x} \notin \mathscr{M}_r$, $\mathscr{L}V(\boldsymbol{x}) < -r$, the second term on the right-hand side of Eq. (11) can be estimated as:

$$\frac{\int_0^t \mathscr{L}V(\boldsymbol{x}_s)\mathbf{1}_{\boldsymbol{x}_s\notin\mathscr{M}_r}\mathrm{d}s}{t} \le -r\frac{\int_0^t \mathbf{1}_{\boldsymbol{x}_s\notin\mathscr{M}_r}\mathrm{d}s}{t} = -r\left[1 - \frac{f_r(t)}{t}\right].$$

In addition, the first term on the right-hand side of Eq. (11) can be estimated as:

$$\frac{\int_0^t \mathscr{L}V(\boldsymbol{x}_s)\mathbf{1}_{\boldsymbol{x}_s\in\mathscr{M}_r}\mathrm{d}s}{t} \le B\frac{\int_0^t \mathbf{1}_{\boldsymbol{x}_s\in\mathscr{M}_r}\mathrm{d}s}{t} = \frac{Bf_r(t)}{t}.$$

On the other hand, using the strong law of the large numbers for the martingale [42] and noticing the boundedness of the trajectory, we obtain that, almost surely in Ω_3,

$$\lim_{t\to+\infty}\frac{1}{t}\int_0^t \mathscr{D}V(\boldsymbol{x}_s)\mathrm{d}\boldsymbol{B}_s = 0,\quad \lim_{t\to+\infty}\frac{1}{t}[V(\boldsymbol{x}_t) - V(\boldsymbol{x}_0)] = 0.$$

All these estimations give that

$$\liminf_{t\to+\infty}\left\{-r\left[1 - \frac{f_r(t)}{t}\right] + \frac{Bf_r(t)}{t}\right\} \ge 0,$$

which leads to a conclusion that $\liminf_{t\to+\infty}\frac{f_r(t)}{t} \ge \frac{r}{r+B}$ almost surely in Ω_3. ■

V. Illustrative Examples

Here, several examples, including the stochastic oscillating dynamics, are provided to demonstrate the efficacy of the above-established criteria.

Example 5.1: First, we investigate how the synchronization dynamics are emergent in the stochastically-coupled FitzHugh-Nagumo neuronal dynamics:

$$\begin{aligned}\mathrm{d}v_i &= \left(v_i - \frac{v_i^3}{3} - w_i + 0.5\right)\mathrm{d}t + k\sum_{j\neq i} a_{ij}(v_j - v_i)\mathrm{d}B_t,\\ \mathrm{d}w_i &= 0.1\,(v_i + 0.7 - 0.8w_i)\,\mathrm{d}t + k\sum_{j\neq i} a_{ij}(w_j - w_i)\mathrm{d}B_t,\end{aligned} \tag{12}$$

where $i = 1, \cdots, N$, each a_{ij} is the connection matrix element, and k is the coupling gain. The purely stochastic couplings in system (12) are often regarded as the diffusion in a fluctuating environment, which can be rewritten as $k\sum_{j=1}^N a_{ij}v_j\mathrm{d}B_t$ and $k\sum_{j=1}^N a_{ij}w_j\mathrm{d}B_t$ in that we set $a_{ii} = -\sum_{j\neq i} a_{ij}$ for all i as usual. To investigate the dynamics of this system, we choose

$$W(v_1, \cdots, v_N, w_1, \cdots, w_N) \triangleq \sum_{i=1}^{N-1}\left[(v_i - v_N)^2 + 10(w_i - w_N)^2\right],$$

$$V(v_1, \cdots, v_N, w_1, \cdots, w_N) \triangleq W^{0.1}.$$

Thus, the diffusion operator with respect to V along the system (12) becomes

$$\begin{aligned}\mathscr{L}V = 0.1W^{-1.9}\Bigg\{&W\sum_{i=1}^{N-1}\left[2(v_i - v_N)^2\left(1 - \frac{v_i^2 + v_iv_N + v_N^2}{3}\right)\right.\\ &\left. - 1.6(w_i - w_N)^2\right] + k^2\Big[W(\boldsymbol{v}^{\mathrm{T}}\boldsymbol{B}^{\mathrm{T}}\boldsymbol{B}\boldsymbol{v} + 10\boldsymbol{w}^{\mathrm{T}}\boldsymbol{B}^{\mathrm{T}}\boldsymbol{B}\boldsymbol{w})\\ &- 1.8(\boldsymbol{v}^{\mathrm{T}}\boldsymbol{B}\boldsymbol{v} + 10\boldsymbol{w}^{\mathrm{T}}\boldsymbol{B}\boldsymbol{w})^2\Big]\Bigg\},\end{aligned}$$

where $\boldsymbol{v}$ and $\boldsymbol{w}$ are vectors defined, respectively, by $\boldsymbol{v} \triangleq [v_1 - v_N, \cdots, v_{N-1} - v_N]$ and $\boldsymbol{w} \triangleq [w_1 - w_N, \cdots, w_{N-1} - w_N]$, and the elements of the matrix $\boldsymbol{B}$ are defined by $b_{ij} \triangleq a_{ij} - a_{Nj}$. Suppose that $\boldsymbol{B}$ satisfies

$$\boldsymbol{x}^{\mathrm{T}}\boldsymbol{B}^{\mathrm{T}}\boldsymbol{B}\boldsymbol{x} - 1.8(\boldsymbol{x}^{\mathrm{T}}\boldsymbol{B}\boldsymbol{x})^2 \le -\alpha < 0 \tag{13}$$

for any $\boldsymbol{x} \in \mathbb{R}^{N-1}$ satisfying $\|\boldsymbol{x}\| = 1$. This thus implies that the set

$$\mathscr{P} \triangleq \Big\{(v_1 - v_N, \cdots, v_{N-1} - v_N, w_1 - w_N, \cdots, w_{N-1} - w_N)\ \Big|\ \mathscr{L}V > 0\Big\}$$

is bounded. According to Theorem 3.4, we obtain $\Omega = \Omega_1 \cup \Omega_2$ a.s., where

$$\Omega_1 = \left\{\lim_{t\to+\infty}[v_i(t) - v_N(t)] = \lim_{t\to+\infty}[w_i(t) - w_N(t)] = 0, \forall i\right\}$$

and

$$\begin{aligned}\Omega_2 = \Big\{&(v_1 - v_N, \cdots, v_{N-1} - v_N, w_1 - w_N, \cdots, w_{N-1} - w_N)\\ &\text{wanders in between the sets circumscribed, respectively,}\\ &\text{by } \mathscr{L}V > 0 \text{ and } \mathscr{L}V < 0\Big\}.\end{aligned}$$

On one hand, a direct computation gives $\mathscr{L}V \le 0$ for $k > \sqrt{2/\alpha}$. Further, with this kind of k, we have $\mathscr{L}V = 0$ if and only if $v_i - v_N = w_i - w_N = 0$ for each i. As such, the set $\mathscr{P}$ as defined above is empty, which further implies that $\mathbb{P}(\Omega_2) = 0$ and $\mathbb{P}(\Omega_1) = 1$. Consequently, provided with $k > \sqrt{2/\alpha}$, the stochastically-coupled neuronal oscillators are synchronized with probability one. On the other hand, for $k < \sqrt{2/\alpha}$, denote two indexes $B(k)$ and $R(k)$, respectively, by

$$\begin{aligned}B(k) &\triangleq \sup_{v_i,\ w_i,\ i=1,\cdots,N} \mathscr{L}V(v_1, \cdots, v_N, w_1, \cdots, w_N),\\ R(k) &\triangleq \sup_{\mathscr{L}V > -B(k)} W(v_1, \cdots, v_N, w_1, \cdots, w_N),\end{aligned} \tag{14}$$

where $B(k)$ is defined in the same manner as B in Theorem 3.9 for a given k. If $B(k) < +\infty$, which will be numerically validated for specific cases, we define two time indices, $T(k)$ and $F(k)$, by:

$$T(k) \triangleq \liminf_{t\to+\infty}\frac{\int_0^t \mathbf{1}_{W\le R(k)}\mathrm{d}s}{t},\quad F(k) \triangleq \liminf_{t\to+\infty}\frac{\int_0^t \mathbf{1}_{\boldsymbol{x}_s\in\mathscr{M}_{B(k)}}\mathrm{d}s}{t}, \tag{15}$$

both of which describe how often the trajectories stay in specified bounded sets. By virtue of Theorem 3.9, we get that

$$T(k) \ge F(k) \ge \frac{1}{2} \tag{16}$$

almost surely for any bounded trajectory of system (12).

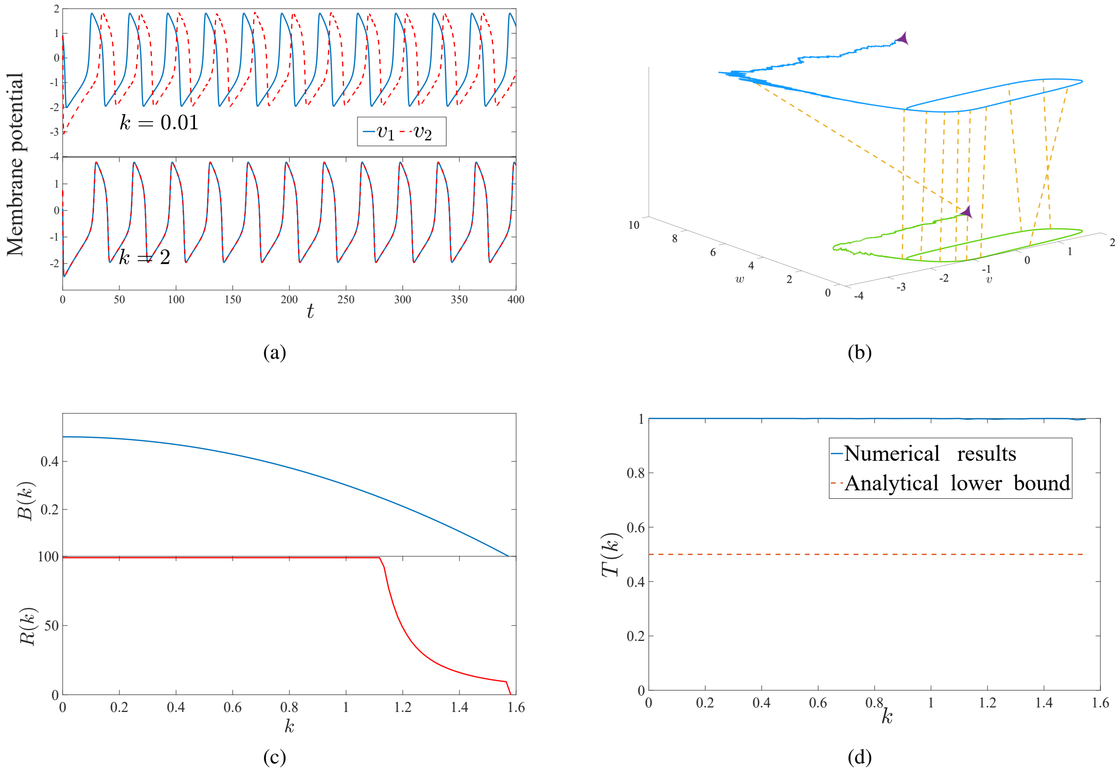

Fig. 1. (a) Unsynchronized and synchronized spiking dynamics of the membrane potential variables of the first and the second neurons in the stochastically-coupled FitzHugh-Nagumo system (12) for different coupling gain k. (b) To display more clearly in the phase space, trajectories of the first two neurons are depicted at different level. The solid (blue and green) lines represent the trajectories of the neurons 1 and 2, respectively. The dashed (yellow) lines represent line connecting different nodes at the same time instants. (c) Two indexes $R(k)$ and $B(k)$, defined in (14), change, respectively, with k. (d) Dependence of the time index for a particular bounded set, $T(k)$, which is defined in Eq. (15), on the noise of coupling k. Here, the time index (the blue solid curve) is calculated as the minimum of 100 random numerical realization of system (12), while the dashed (red) line stands for the analytical lower bound obtained from (16).

Now, we investigate the above stochastically-coupled system more specifically. We select the coupling settings particularly as: $N = 100$, $a_{ij} = 1$ for $i \neq j$ and $1 \leq j \leq 99$, $a_{i,100} = -98$ for $1 \leq i \leq 99$, $a_{ii} = 0$ for $1 \leq i \leq 99$, and $a_{100,100} = -99$. For these stochastic couplings, setting $\alpha = 0.8$ makes the inequality in (13) valid. As is shown in the lower panel of Fig. 1(a), the system displays synchronized dynamics as the sufficient condition $k > \sqrt{2.5}$ for stability is satisfied. However, as displayed in the upper panel of Fig. 1(a) and in Fig. 1(b) as well, unsynchronized dynamics could be observed for sufficiently small k with $0 < k < \sqrt{2.5}$. Next, we show numerically in Fig. 1(c) that $B(k) < +\infty$ and $R(k) < +\infty$ for $0 < k < \sqrt{2.5}$. Thus, according to the above estimations obtained in (16), we have $T(k) \geq \frac{1}{2}$ almost surely for any bounded trajectory. Numerical results presented in Fig. 1(d) confirm this analytical estimation on how often the bounded trajectory stay in the considered set. To be candid, the numerical result for $T(k)$ is much larger than $1/2$, which also indicates that our analytical estimation could be improved further. □

Example 5.2: We consider the stochastic synchronization among the N coupled bursting neurons. The dynamics are described by the stochastically-coupled Hindmarsh-Rose oscillators as:

$$\begin{aligned}
\mathrm{d}x_i &= (y_i - x_i^3 + 3x_i^2 - z_i + 3)\mathrm{d}t + k\sum_{j\neq i} a_{ij}(x_j - x_i)\mathrm{d}B_t,\\
\mathrm{d}y_i &= (1 - 5x_i^2 - y_i)\mathrm{d}t + k\sum_{j\neq i} a_{ij}(y_j - y_i)\mathrm{d}B_t,\\
\mathrm{d}z_i &= 0.01(4x_i + 6.4 - z_i)\mathrm{d}t + k\sum_{j\neq i} a_{ij}(z_j - z_i)\mathrm{d}B_t,
\end{aligned}\tag{17}$$

where k, in front of the stochastic terms, is the coupling strength and each uncoupled neuron with the parameters specified in the vector field displays bursting dynamics as reported in the literature. Here, we set $W(x_i, y_i, z_i) \triangleq \sum_{i=1}^{N}\left[(x_i - \overline{x})^2 + (y_i - \overline{y})^2 + (z_i - \overline{z})^2\right]$ and $V(x_i, y_i, z_i) \triangleq W^{0.1}(x_i, y_i, z_i)$, where

$$\overline{x} = \frac{1}{N}\sum_{i=1}^{N} x_i, \quad \overline{y} = \frac{1}{N}\sum_{i=1}^{N} y_i, \quad \overline{z} = \frac{1}{N}\sum_{i=1}^{N} z_i$$

represent the mean fields of the corresponding states of the coupled neurons. For simplicity, we set $\boldsymbol{X}_i \triangleq [x_i, y_i, z_i]^{\mathrm{T}}$, the mean field vector $\overline{\boldsymbol{X}} \triangleq [\overline{x}, \overline{y}, \overline{z}]^{\mathrm{T}}$, and the vector field function

$$\boldsymbol{F}(\boldsymbol{X}_i) \triangleq [y - x^3 + 3x^2 - z + 3, 1 - 5x^2 - y, 0.01(4x + 6.4 - z)]^{\mathrm{T}}.$$

Furthermore, we assume that the connection matrix $\boldsymbol{A} = \{a_{ij}\}$ are symmetric and satisfies $a_{ii} = -\sum_{j\neq i} a_{ij}$. With these settings, the diffusion operator with respect to $V(\boldsymbol{X}_i)$ along system (17) becomes

$$
\begin{aligned}
\mathscr{L}V(\boldsymbol{X}_i) = 0.1W^{-1.9} \Bigg\{ & 2W \sum_{i=1}^{N} \left\langle \boldsymbol{X}_i - \overline{\boldsymbol{X}}, \boldsymbol{F}(\boldsymbol{X}_i) - \boldsymbol{F}(\overline{\boldsymbol{X}}) \right\rangle \\
& + k^2 \Bigg[W \left\langle \sum_{j=1}^{N} a_{ij}(\boldsymbol{X}_j - \overline{\boldsymbol{X}}), \sum_{j=1}^{N} a_{ij}(\boldsymbol{X}_j - \overline{\boldsymbol{X}}) \right\rangle \\
& -1.8 \left(\sum_{i=1}^{N} \left\langle \boldsymbol{X}_i - \overline{\boldsymbol{X}}, \sum_{j=1}^{N} a_{ij}(\boldsymbol{X}_j - \overline{\boldsymbol{X}}) \right\rangle \right)^2 \Bigg] \Bigg\}
\end{aligned}
$$

with $\langle \cdot, \cdot \rangle$ representing the product of two given vectors. Here, we set an assumption that the matrix $\boldsymbol{A}$ satisfies

$$
\boldsymbol{x}^{\mathrm{T}} \boldsymbol{A}^{\mathrm{T}} \boldsymbol{A} \boldsymbol{x} - 1.8(\boldsymbol{x}^{\mathrm{T}} \boldsymbol{A} \boldsymbol{x})^2 \leq -\alpha < 0 \tag{18}
$$

for any $\boldsymbol{x} \in \mathbb{R}^n$ with $\|\boldsymbol{x}\| = 1$ and $[1, 1, \cdots, 1]\boldsymbol{x} = 0$. We also have the following estimations:

$$
\begin{aligned}
& \left\langle \boldsymbol{X}_i - \overline{\boldsymbol{X}}, \boldsymbol{F}(\boldsymbol{X}_i) - \boldsymbol{F}(\overline{\boldsymbol{X}}) \right\rangle \\
& = (x_i - \overline{x})(y_i - \overline{y}) - (x_i - \overline{x})^2 \left(x_i^2 + x_i \overline{x} + \overline{x}^2 \right) \\
& \quad + 3(x_i - \overline{x})^2 (x_i + \overline{x}) - 5(x_i - \overline{x})(x_i + \overline{x})(y_i - \overline{y}) - (y_i - \overline{y})^2 \\
& \quad - (x_i - \overline{x})(z_i - \overline{z}_i) + 0.04(x_i - \overline{x})(z_i - \overline{z}) - 0.01(z_i - \overline{z})^2 \\
& \leq 31 \cdot |x_i - \overline{x}| \cdot |y_i - \overline{y}| + 18(x_i - \overline{x})^2 - (y_i - \overline{y})^2 \\
& \quad + 0.96 \cdot |x_i - \overline{x}| \cdot |z_i - \overline{z}_i| \\
& \leq 10(x_i - \overline{x})^2 + 29(y_i - \overline{y})^2 + 18(x_i - \overline{x})^2 - (y_i - \overline{y})^2 \\
& \quad + 0.5(x_i - \overline{x})^2 + 0.5(z_i - \overline{z})^2 \\
& \leq 29 \left[(x_i - \overline{x})^2 + (y_i - \overline{y})^2 + (z_i - \overline{z})^2 \right].
\end{aligned}
$$

Here, we use the boundedness of the trajectory close to the synchronization manifold of system (17) (i.e., $|x_i| \leq 3$ and $|\overline{x}| \leq 3$), which we numerically demonstrate in Fig. 2(a). Hence, together with the above assumption and the estimations, the diffusion operator computed above becomes:

$$
\mathscr{L}V(\boldsymbol{X}_i) \leq 0.1W^{-0.9} \left[58W - \alpha k^2 W \right]
$$

in the vicinity of the synchronization manifold. Thus, for $k \geq k_c \triangleq \sqrt{58/\alpha}$, we have $\mathscr{L}V \leq 0$ near and within the synchronization manifold. Therefore, in light of Theorem 3.4, we can achieve stochastic bursting synchronization, i.e.,

$$
\lim_{t \to +\infty} x_i(t) - \overline{x}(t) = \lim_{t \to +\infty} y_i(t) - \overline{y}(t) = \lim_{t \to +\infty} z_i(t) - \overline{z}(t) = 0
$$

for $k \geq k_c$ and $\forall i$. On the other hand, for $0 < k \leq k_c$, denote two indexes $B(k)$ and $R(k)$, respectively, by

$$
B(k) \triangleq \sup_{|x_i| \leq 3, \forall i} \mathscr{L}V(\boldsymbol{X}_i), \quad R(k) \triangleq \sup_{\mathscr{L}V > -B(k),\ |x_i| \leq 3, \forall i} W(\boldsymbol{X}_i),
$$

whose boundedness is validated numerically [see Fig. 2(b)]. Also, for each k, we use the notations for $T(k)$ and $F(k)$, the same as those defined in (15). Hence, by virtue of Theorem 3.9, we get the following estimation:

$$
T(k) \geq F(k) \geq \frac{1}{2}, \tag{19}
$$

almost surely for any bounded trajectory of system (17).

Now, we investigate the above stochastically-coupled bursting neurons more specifically. We select the coupling matrix $\boldsymbol{A}$ particularly as: $N = 100$, $a_{ij} = 1$ for $i \neq j$ and the diagonal elements $a_{ii} = -99$ for $1 \leq i \leq 100$. Using these stochastic couplings and $\alpha = 0.8$ makes the inequality in (18) valid. This further indicates that $k_c = \sqrt{72.5}$. As is shown in the lower panel of Fig. 2(a), the system (17) using only stochastic couplings can display synchronized bursting dynamics as the sufficient condition $k > k_c$ is satisfied. However, as displayed in the upper panel of Fig. 2(a) as well, unsynchronized dynamics could be observed for a sufficiently small k violating $k > k_c$. Next, we show numerically in Fig. 2(b) that $B(k) < +\infty$ and $R(k) < +\infty$ for $0 < k < k_c$. Thus, according to the above estimations obtained in (19), we have $T(k) \geq \frac{1}{2}$ almost surely for any bounded trajectory. Numerical results presented in Fig. 2(c) confirm this analytical estimation on how often the bounded trajectory stay in the considered set. □

The final example provides a more delicate application of our analytical results.

Example 5.3: Finally, we consider the following noise-perturbed oscillator in a normal form as:

$$
\mathrm{d}z_t = \left(\mathrm{i} + 1 - |z_t|^2 \right) z_t \mathrm{d}t + \left(\mathrm{i}w + C - |z_t|^2 \right) z_t \mathrm{d}B_t, \tag{20}
$$

where all the deterministic coefficients are supposed to be perturbed by the external noise. Here, $z_t \in \mathbb{C}$ is a complex-valued state, $\mathrm{i}^2 = -1$, and $C \geq 1$, $1 \geq w \geq 0$ are tunable parameters.

Now, we select $V(z) \triangleq |z|^2$ and $W_\alpha(z) \triangleq |z|^{2\alpha}$ with a sufficiently small $\alpha > 0$. Hence, operations of $\mathscr{L}$ and $\mathscr{D}$, respectively, on V and W_α along system (20) yield:

$$
\begin{aligned}
& \mathscr{L}V(z) = 2|z|^2 \left(1 - |z|^2 \right) + |z|^2 \left(C - |z|^2 \right)^2 + w^2 |z|^2, \\
& \mathscr{D}V(z) = 2|z|^2 \left(C - |z|^2 \right),
\end{aligned}
$$

and

$$
\begin{aligned}
& \mathscr{L}W_\alpha(z) = \alpha |z|^{2\alpha} \left[2 \left(1 - |z|^2 \right) + w^2 + (2\alpha - 1) \left(C - |z|^2 \right)^2 \right], \\
& \mathscr{D}W_\alpha(z) = 2\alpha |z|^{2\alpha} \left(C - |z|^2 \right).
\end{aligned}
$$

Thus, we have

$$
\begin{aligned}
& \{ z \in \mathbb{C} \mid \mathscr{L}V(z) = 0,\ \mathscr{D}V(z) = 0 \} \\
& \quad = \{ z \in \mathbb{C} \mid \mathscr{L}W_\alpha(z) = 0,\ \mathscr{D}W_\alpha(z) = 0 \} = \{0\}
\end{aligned}
$$

for $C \neq 1 + \frac{1}{2}w^2$, and

$$
\begin{aligned}
& \{ z \in \mathbb{C} \mid \mathscr{L}V(z) = 0,\ \mathscr{D}V(z) = 0 \} = \{ z \in \mathbb{C} \mid \\
& \quad \mathscr{L}W_\alpha(z) = 0,\ \mathscr{D}W_\alpha(z) = 0 \} = \{0\} \cup \left\{ z \in \mathbb{C} \mid |z| = \sqrt{C} \right\}
\end{aligned}
$$

for $C = 1 + \frac{1}{2}w^2$. Also notice that $\left\{ z \in \mathbb{C} \,\middle|\, \mathscr{L}W_\alpha(z) > 0 \right\}$ is a bounded set for sufficiently small α.

First, we use the function $V(z)$. For $C > 1 + \frac{1}{2}w^2$, we take a sufficiently small $\delta > 0$ and construct a set as

$$
\left\{ z \in \mathbb{C} \,\middle|\, C - \delta \leq |z|^2 \leq C \right\}.
$$

In this set, we have

$$
|\mathscr{D}V(z)| = 2|z|^2 \left(C - |z|^2 \right) \leq 2|C|^2 \left(C - |z|^2 \right) = 2|C|^2 \left[C - V(z) \right],
$$

and

$$
\begin{aligned}
& |\mathscr{L}V(z)| = |z|^2 \left(C - |z|^2 \right)^2 + |z|^2 \left(2 - 2|z|^2 + w^2 \right) \\
& \quad \leq \left[2 + w^2 - 2(C - \delta) \right] (C - \delta) + \delta^2 C^2 \leq 0 \leq 2 \left[C - V(z) \right].
\end{aligned}
$$

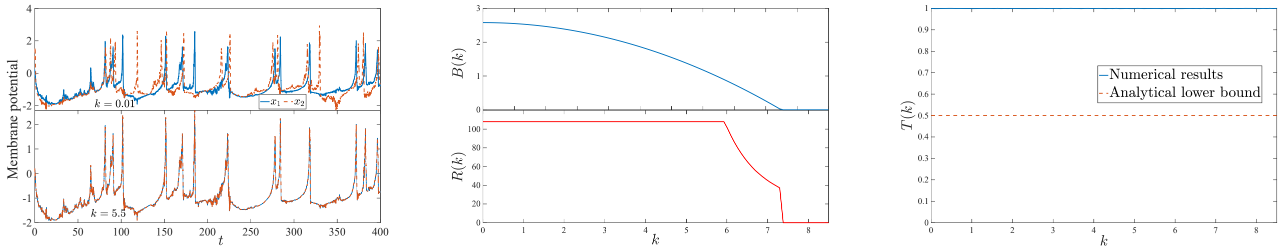

(a) (b) (c)

Fig. 2. (a) Unsychronized and synchronized bustring dynamics of the membrane potential variables of the two oscillators that are described by the stochastically coupled Hindmarsh-Rose neurons (17) for different coupling gain k. (b) Both $R(k)$ and $B(k)$ change with k, respectively, for the coupled system (17). (c) Dependence of the time index for a particular bounded set, $T(k)$, on the noise of coupling k. Here, the time index(the blue solid curve) is calculated as the minimum of 100 random numerical realization of system (12), while the dashed (red) line stands for the analytical lower bound obtained from (19).

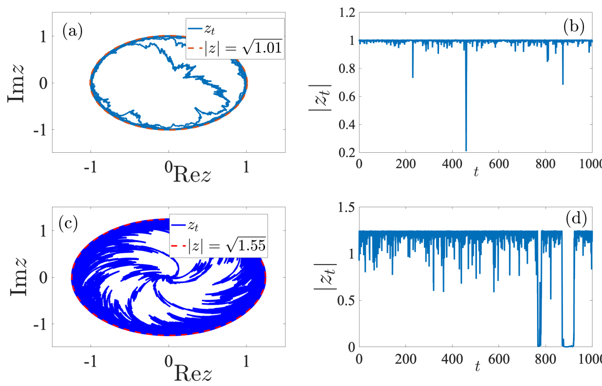

Fig. 3. Stochastic and complex dynamics of system (20) for different parameters. (a),(c) The evolutionary trajectories on the complex plane. The solid (blue) lines represent the trajectories of system (20), and the invariant set $\left\{z \in \mathbb{C} \,\middle|\, |z|^2 \le C\right\}$ analytically obtained is circumstanced by the dashed (red) circles. (b),(d) The dynamics of the norm of the complex valued state $|z_t|$ changes with t. Here, the parameters are set as $w = 0$, $C = 1.01$ for (a)-(b), and $w = 1$, $C = 1.55$ for (c)-(d).

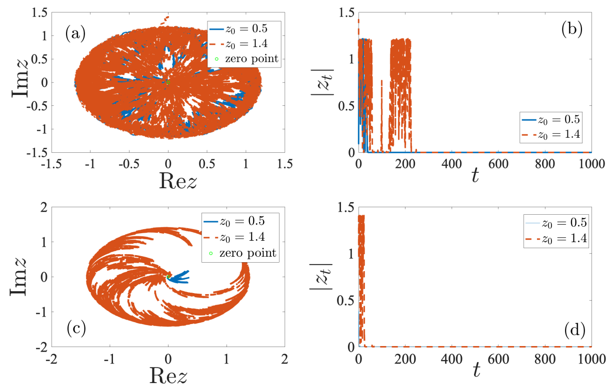

Fig. 4. Stochastic convergent dynamics of (20) with different initial values. (a),(c) The trajectories convergent to the origin, highlighted by the green point, on the complex plane. The solid (blue) and dashed (red) lines represent the trajectories of (20) with different initial values. (b),(d) The convergent dynamics of the norm $|z_t|$ changes with t. Here, the parameters are $w = 0$, $C = 1.51$ for (a)-(b), and $w = 1$, $C = 2.01$ for (c)-(d).

As such, the constants δ and $k_{1,2}$, as required in the estimations of Theorem 3.1, have been found. Therefore, it follows that $\{z \in \mathbb{C} \mid |z|^2 \le C\}$ is an invariant set, which is further numerically shown in Fig. 3.

Moreover, to further use the function $W_\alpha(z)$ appropriately, we, based on $\mathscr{L}W_\alpha(z)$, set a function as

$$f_\alpha(x) \triangleq 2(1-x) + w^2 + (2\alpha - 1)(C-x)^2,$$

and we obtain its derivative as $f'_\alpha(x) = -2 + (2\alpha - 1)(x - C)$, where $\alpha > 0$ is sufficiently small. Thus, we get that $f'_\alpha(x) > 0$ on $(0, C + \frac{1}{2\alpha-1})$ and that $f'_\alpha(x) < 0$ on $(0, C + \frac{1}{2\alpha-1})$. This directly implies that $f_\alpha(x)$ attains its maximum $f_\alpha^{\max} = 2 - 2C - \frac{1}{2\alpha-1} + w^2$ at $x = C + \frac{1}{2\alpha-1}$.

Case I: $C > 1.5 + \frac{1}{2}w^2$. For each C, there exists $\alpha > 0$ such that $f_\alpha^{\max} = 2 - 2C - \frac{1}{2\alpha-1} + w^2 < 0$, which further implies $f_\alpha(x) < f_\alpha^{\max} < 0$ for all $x \ge 0$. Hence, we get $\mathscr{L}W_\alpha(z) \le 0$ for all $z \in \mathbb{C}$, so that Ω_2 defined in Theorem 3.4 is an empty set. Consequently, according to Theorem 3.4, we have $\mathbb{P}(\Omega_1) = \mathbb{P}(\Omega) = 1$. This indicates $\lim_{t\to+\infty} z_t = 0$ a.s., which is numerically displayed in Fig. 4.

Case II: $1 + \frac{1}{2}w^2 < C < 1.5 + \frac{1}{2}w^2$. Denote by $s_{1,\alpha}$ and $s_{2,\alpha}$ the two roots for the equation $f_\alpha(x) = 0$ with $s_{1,\alpha} > s_{2,\alpha}$ and $s_{1,\alpha} < C$ for $C > 1 + \frac{1}{2}w^2$. Thus, we compute as follows:

$$\left\{z \in \mathbb{C} \,\middle|\, \mathscr{L}W_\alpha(z) > 0\right\} = \left\{z \in \mathbb{C} \,\middle|\, s_{2,\alpha} < |z| < s_{1,\alpha}\right\},$$
$$\left\{z \in \mathbb{C} \,\middle|\, \mathscr{L}W_\alpha(z) < 0\right\} = \left\{z \in \mathbb{C} \,\middle|\, |z| > s_{1,\alpha} \text{ or } 0 < |z| < s_{2,\alpha}\right\},$$

for $\sqrt{2 + w^2} < C < 1.5 + \frac{1}{2}w^2$, and

$$\left\{z \in \mathbb{C} \,\middle|\, \mathscr{L}W_\alpha(z) > 0\right\} = \left\{z \in \mathbb{C} \,\middle|\, 0 < |z| < s_{1,\alpha}\right\},$$
$$\left\{z \in \mathbb{C} \,\middle|\, \mathscr{L}W_\alpha(z) < 0\right\} = \left\{z \in \mathbb{C} \,\middle|\, |z| > s_{1,\alpha}\right\}.$$

for $1 + \frac{w^2}{2} < C < \sqrt{2 + w^2}$. Hence, according to Theorem 3.4, the trajectory of system (20) almost surely enters the circle $\left\{z \in \mathbb{C} \,\middle|\, |z| = \sqrt{C}\right\}$. This results in a *conclusion* that $\Omega = \Omega_1 \cup \Omega_2$ a.s., where $\Omega_1 = \left\{\omega \,\middle|\, \lim_{t\to+\infty} z_t = 0\right\}$ and

$$\Omega_2 = \left\{\omega \,\middle|\, z_t \text{ oscillates between } \mathscr{A}_+ \text{ and } \mathscr{A}_- \text{ infinite times}\right\}.$$

Here, we denote by $\mathscr{A}_+ \triangleq \left\{z \in \mathbb{C} \,\middle|\, \mathscr{L}W_\alpha(z) > 0\right\}$, whose boundedness has been pointed above, and denote by

$$\mathscr{A}_- \triangleq \left\{z \in \mathbb{C} \,\middle|\, \mathscr{L}W_\alpha(z) < 0\right\} \cap \left\{z \in \mathbb{C} \,\middle|\, |z| < \sqrt{C}\right\}.$$

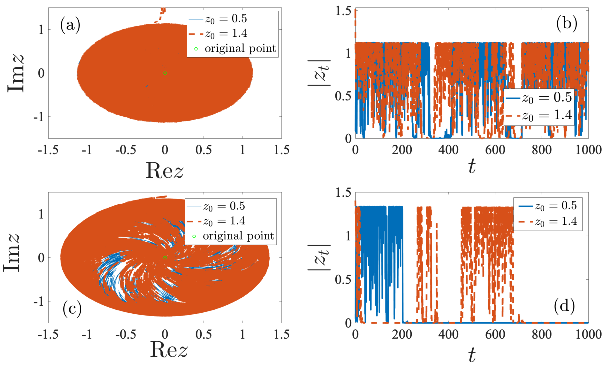

Fig. 5. Stochastic complex dynamics of system (20) starting from different initial values. (a),(c) The trajectories on the complex plane, where the green point represents the origin and the solid (blue) and the dashed (red) lines represent the trajectories with different initial values. (b),(d) The wandering dynamics of the norm $|z_t|$. Here, the parameters are set as $w = 0$, $C = 1.3$ for (a)-(b), and $w = 1$, $C = 1.8$ for (c)-(d).

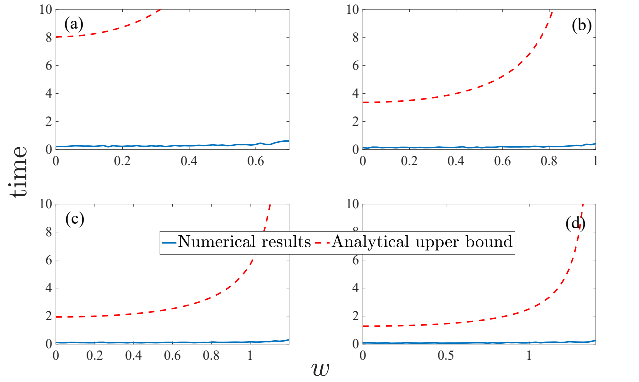

Fig. 6. Dependence of the mean value, $\mathbb{E}[\mu_{w,C}]$, on the parameters w and C. The solid (blue) curves correspond to the numerical evaluation of $\mu_{w,C}$, which is counted as the average over the 100 random realizations of system (20). The dashed (red) curves correspond to the upper bound obtained from the analytical estimation specified in (21). Here, C=2 (a), C=2.5 (b), C=3 (c), C=3.5 (d), and the initial values are uniformly and randomly chosen from the circle $\left\{z \in \mathbb{C} \,\middle|\, |z| = 10\right\}$.

Finally, we are to estimate the time that a trajectory uses to enter the circle $\left\{z \in \mathbb{C} \,\middle|\, |z| = \sqrt{C}\right\}$ from any initial value $z_0 > \sqrt{C}$. To this end, denote this time by

$$\mu_{w,C} \triangleq \inf\left\{t > 0 \,\middle|\, |z_t| \le \sqrt{C}\right\},$$

and select $U(z) \triangleq \log|z|$ where U is defined in the set $\left\{z \in \mathbb{C} \,\middle|\, |z| \ge \sqrt{C}\right\}$. Hence, a direct computation yields:

$$\mathscr{L}U(z) = 1 + \frac{w^2}{2} - |z|^2 - \frac{\left(C - |z|^2\right)^2}{2}$$

and

$$p(r) = \frac{1}{2}\log\left(\sqrt{3 + w^2 + 2r - 2C} + C - 1\right).$$

Consequently, according to Theorem 3.8, we obtain the estimation for the average of the time as:

$$\mathbb{E}[\mu_{w,C}] \le \int_{r_1}^{r_2} \frac{p'(s)}{s}\mathrm{d}s, \tag{21}$$

where the upper and the lower bounds $r_{1,2}$ satisfy that $p(r_1) = \frac{1}{2}\log C$ and $p(r_2) = \log|z_0|$. In Fig. 6, both the numerical results and the results obtained using (21) are shown, illustrating the usefulness of our analytical criteria.

VI. Concluding Remarks

This article has developed several versions of invariance principle for continuous-time and autonomous differential equations with stochastic perturbations. Indeed, this article has not only established a local invariance principle, but also provided a generalized global invariance principle which allows the sign of the diffusion operator to be positive in a bounded region. Furthermore, the article has provided a time estimation for the trajectory entering or staying in a particular set. Finally, the article has used several examples, including the stochastic neural dynamics, to demonstrate the efficacy of the established analytical criteria.

For future directions, a few issues remain open. For example, if the set for which the diffusion operator along the system is unbounded, how can we describe the long-term behaviors of the trajectories produced by the stochastic dynamical systems? Besides, as we can see in Examples 5.1-5.3, the time estimation for the orbit entering or staying in a particular bounded set is fairly away from the corresponding numerical result. This naturally suggests that a more precise estimation is in demand. Practically, applications of the current or/and the developing results to more physical, biological, and ecological models are highly expected.

VII. Appendix

Lemma 7.1: [1] Let A_t^1 and A_t^2 be two non-decreasing adapted processes with $A_0^1 = A_0^2 = 0$. Let also Z be a semimartingale with initial state $\mathbb{E}Z_0 < +\infty$ and

$$Z_t = Z_0 + A_t^1 - A_t^2 + M_t, \quad t \ge 0,$$

where M is a local martingale with $M_0 = 0$. If A_t^1 and Z_t are both continuous processes, then

$$\left\{\lim_{t\to+\infty} A_t^1 < +\infty\right\} \cap \left\{\inf_{t\ge 0} Z_t > -\infty\right\} \subseteq \left\{\lim_{t\to\infty} Z_t \text{ exists finitely}\right\}$$
$$\cap \left\{\lim_{t\to+\infty} A_t^2 < +\infty\right\} \cap \left\{\lim_{t\to\infty} M_t \text{ exists finitely}\right\} \text{ a.s..}$$

Proof of Lemma 7.1. Denote by stopping times $\kappa_n \triangleq \inf\left\{t \ge 0 \,\middle|\, A_t^1 - Z_t \ge n\right\}$. Due to the continuity of both A_t^1 and Z_t, we obtain $A_{t\wedge\kappa_n}^1 - Z_{t\wedge\kappa_n} \le \max\{n, -Z_0\}$. Furthermore, we have

$$\begin{aligned} M_{t\wedge\kappa_n} &= (Z_{t\wedge\kappa_n} - A_{t\wedge\kappa_n}^1) + A_{t\wedge\kappa_n}^2 - Z_0 \\ &\ge \min\{-n, Z_0\} - Z_0 \ge \min\{-n - Z_0, 0\}. \end{aligned}$$

According to Fatou's lemma [58], we conclude that $M_{t\wedge\kappa_n}$ is a supermartingale with an integrable lower bound. Thus, using

[1] Reference [30] only considered the situation of $Z_t \ge 0$; however, we generalize it to a situation where the trajectory of Z_t has a lower bound (but not necessarily in uniform manner). The proof for this Lemma is inspired by those arguments used in [30].

the well-known Doob Martingale Convergence Theorem [30] yields that the limit $\lim_{t\to+\infty} M_{t\wedge\kappa_n}$ exists finitely almost surely.

Moreover, $\lim_{t\to+\infty} M_t$ exists finitely almost surely in the set $\{\kappa_n = +\infty\}$, which further indicates that $\sup_{t>0} M_t < +\infty$ almost surely. Therefore, in the set $\{\kappa_n = +\infty\}$, $A_t^2 = Z_0 + (A_t^1 - Z_t) + M_t \le Z_0 + \max\{n, -Z_0\} + \sup_{t>0} M_t$. This estimation about the monotonous process A_t^2 implies the existence of the limit $\lim_{t\to+\infty} A_t^2$ in the set $\{\kappa_n = +\infty\}$. Since

$$\left\{\lim_{t\to+\infty} A_t^1 < +\infty\right\} \cap \left\{\omega : \inf_{t\ge0} Z_t > -\infty\right\} \subseteq \cup_{n=1}^{+\infty}\{\kappa_n = +\infty\},$$

we derive that

$$\left\{\lim_{t\to+\infty} A_t^1 < +\infty\right\} \cap \left\{\inf_{t\ge0} Z_t > -\infty\right\} \subseteq \left\{\lim_{t\to+\infty} A_t^2 < +\infty\right\}$$

$$\cap \left\{\lim_{t\to\infty} M_t \text{ exists finitely}\right\} \text{ a.s..}$$

Finally, the boundedness of the non-decreasing process A_t^1 also implies the convergence of it, which further suggests the convergence of Z_t. This completes the proof. ∎

Lemma 7.2: Suppose that $h(\boldsymbol{x})$ is a nonnegative continuous function defined on $\mathbb{R}^p$. Then, for the solution of system (1),

$$\Lambda \triangleq \left\{\sup_{t>0}\|\boldsymbol{x}_t\| < +\infty\right\} \cap \left\{\int_0^{+\infty} h(\boldsymbol{x}_t)\mathrm{d}t < +\infty\right\}$$
$$\subseteq \left\{\lim_{t\to+\infty} h(\boldsymbol{x}_t) = 0\right\} \text{ a.s..}$$

Proof of Lemma 7.2 [2]. The set Λ can be written as $\Lambda = \cup_{n=1}^{+\infty}\Lambda_n$, where $\Lambda_n \triangleq \left\{\sup_{t>0}\|\boldsymbol{x}_t\| < n\right\} \cap \left\{\int_0^{+\infty} h(\boldsymbol{x}_t)\mathrm{d}t < n\right\}$. It suffices to show that, for each n, the probability $\mathbb{P}[\Lambda_n \cap \{\limsup_{t\to+\infty} h(\boldsymbol{x}_t) > 0\}] = 0$. If this is not the case, there exists a number $\epsilon > 0$ such that $\mathbb{P}[\Lambda_n \cap \{\limsup_{t\to+\infty} h(\boldsymbol{x}_t) > 2\epsilon\}] > \epsilon$. Denote a stopping time by $\zeta = \inf\left\{t > 0 \middle| \|\boldsymbol{x}_t\| \ge n \text{ or } \int_0^t h(\boldsymbol{x}_s)\mathrm{d}s \ge n\right\}$. This thus leads to that $\mathbb{P}[\{\zeta = +\infty\} \cap \{\limsup_{t\to+\infty} h(\boldsymbol{x}_t) > 2\epsilon\}] > \epsilon$. In addition, we have

$$\mathbb{E}\left[\int_0^{+\infty} h(\boldsymbol{x}_t)\mathrm{d}t;\quad \zeta = +\infty\right] \le n. \tag{22}$$

Now, we define an increasing sequence of stopping times, respectively, by

$$T_1 \triangleq \inf\{t \ge 0 | h(\boldsymbol{x}_t) \ge \epsilon\},\quad T_2 \triangleq \inf\{t \ge T_1 | h(\boldsymbol{x}_t) \le \frac{\epsilon}{2}\},\cdots$$
$$T_{2m-1} \triangleq \inf\{t \ge T_{2m-2} | h(\boldsymbol{x}_t) \ge \epsilon\},$$
$$T_{2m} \triangleq \inf\{t \ge T_{2m-1} | h(\boldsymbol{x}_t) \le \frac{\epsilon}{2}\},\cdots$$

[2]The proof for this Lemma used the arguments analogous to those used in [22], [31].

Therefore, $h(\boldsymbol{x}_t) \ge \epsilon/2$ for $T_{2i-1} < t < T_{2i}$, which, in light of Fubini's Theorem [58], allows us to estimate the expectation in (22) as

$$\begin{aligned}
n &\ge \mathbb{E}\left[\int_0^{+\infty} h(\boldsymbol{x}_t)\mathrm{d}t;\quad \zeta = +\infty\right] \\
&\ge \mathbb{E}\left[\sum_{i=1}^{+\infty}\int_{T_{2i-1}}^{T_{2i}} h(\boldsymbol{x}_t)\mathrm{d}t;\quad \zeta = +\infty\right] \\
&= \sum_{i=1}^{+\infty}\mathbb{E}\left[\int_{T_{2i-1}}^{T_{2i}} h(\boldsymbol{x}_t)\mathrm{d}t;\quad \zeta = +\infty, T_{2i-1} = +\infty\right] \\
&\ge \sum_{i=1}^{+\infty}\mathbb{E}\left[\int_{T_{2i-1}}^{T_{2i}} \frac{\epsilon}{2}\mathrm{d}t;\quad \zeta = +\infty, T_{2i-1} < +\infty\right] \\
&= \frac{\epsilon}{2}\sum_{i=1}^{+\infty}\mathbb{E}\Big[T_{2i} - T_{2i-1};\quad \zeta = +\infty, T_{2i-1} < +\infty\Big].
\end{aligned} \tag{23}$$

To further estimate the expectations of the differences between the states at different stopping times, we, using Doob's martingale inequality [30], compute as

$$\begin{aligned}
&\mathbb{E}\left[\sup_{0\le t\le T}\|\boldsymbol{x}_{\zeta\wedge(T_{2i-1}+t)} - \boldsymbol{x}_{\zeta\wedge T_{2i-1}}\|^2;\ \zeta\wedge T_{2i-1} < +\infty\right] \\
&= \mathbb{E}\Bigg[\sup_{0\le t\le T}\left\|\int_{\zeta\wedge T_{2i-1}}^{\zeta\wedge(T_{2i-1}+t)} \boldsymbol{f}(\boldsymbol{x}_s)\mathrm{d}s + \int_{\zeta\wedge T_{2i-1}}^{\zeta\wedge(T_{2i-1}+t)} \boldsymbol{g}(\boldsymbol{x}_s)\mathrm{d}\boldsymbol{B}_s\right\|^2; \\
&\qquad \zeta\wedge T_{2i-1} < +\infty\Bigg] \\
&\le 2\mathbb{E}\left[\sup_{0\le t\le T}\left\|\int_{\zeta\wedge T_{2i-1}}^{\zeta\wedge(T_{2i-1}+t)} \boldsymbol{f}(\boldsymbol{x}_s)\mathrm{d}s\right\|^2;\quad \zeta\wedge T_{2i-1} < +\infty\right] \\
&\quad + 2\mathbb{E}\left[\sup_{0\le t\le T}\left\|\int_{\zeta\wedge T_{2i-1}}^{\zeta\wedge(T_{2i-1}+t)} \boldsymbol{g}(\boldsymbol{x}_s)\mathrm{d}\boldsymbol{B}_s\right\|^2;\quad \zeta\wedge T_{2i-1} < +\infty\right] \\
&\le 2\mathbb{E}\left[\sup_{0\le t\le T}\left\|\int_{\zeta\wedge T_{2i-1}}^{\zeta\wedge(T_{2i-1}+t)} \boldsymbol{f}(\boldsymbol{x}_s)\mathrm{d}s\right\|^2;\quad \zeta\wedge T_{2i-1} < +\infty\right] \\
&\quad + 8\mathbb{E}\left[\sup_{0\le t\le T}\int_{\zeta\wedge T_{2i-1}}^{\zeta\wedge(T_{2i-1}+t)} \|\boldsymbol{g}(\boldsymbol{x}_s)\|^2\mathrm{d}s;\quad \zeta\wedge T_{2i-1} < +\infty\right] \\
&\le 2\mathbb{E}\left[M_n^2 t^2;\ \zeta\wedge T_{2i-1} < +\infty\right] + 8\mathbb{E}\left[M_n^2 t;\ \zeta\wedge T_{2i-1} < +\infty\right] \\
&\le 2M_n^2 t(t+4),
\end{aligned}$$

where $M_n = \sup_{\|\boldsymbol{x}\|\le n}\{\|\boldsymbol{f}(\boldsymbol{x})\|, \|\boldsymbol{g}(\boldsymbol{x})\|\} < +\infty$. The consistent continuity of h in any compact set ensures the existence of $\delta > 0$ such that, for any $\|\boldsymbol{x}\| \le n$ and $\|\boldsymbol{y}\| \le n$ with $\|\boldsymbol{x}-\boldsymbol{y}\| \le \delta$, we have $|h(\boldsymbol{x}) - h(\boldsymbol{y})| \le \frac{\epsilon}{2}$. By using Chebyshev's Inequality [30], we obtain

$$\begin{aligned}
&\mathbb{P}\left[\sup_{0\le t\le T}\|\boldsymbol{x}_{\zeta\wedge(T_{2i-1}+t)} - \boldsymbol{x}_{\zeta\wedge T_{2i-1}}\| \ge \delta; \zeta\wedge T_{2i-1} < +\infty\right] \\
&\le \frac{2M_n^2 t(t+4)}{\delta^2},
\end{aligned}$$

which further indicates that

$$\begin{aligned}
&\mathbb{P}\left[T_{2i}-T_{2i-1}\le t;\ \zeta=+\infty,\ T_{2i-1}<+\infty\right]\\
\le&\mathbb{P}\left[\sup_{0\le t\le T}\|\boldsymbol{x}_{\zeta\wedge(T_{2i-1}+t)}-\boldsymbol{x}_{\zeta\wedge T_{2i-1}}\|\ge\delta;\ \zeta=+\infty,\ T_{2i-1}<+\infty\right]\\
\le&\mathbb{P}\left[\sup_{0\le t\le T}\|\boldsymbol{x}_{\zeta\wedge(T_{2i-1}+t)}-\boldsymbol{x}_{\zeta\wedge T_{2i-1}}\|\ge\delta;\ \zeta\wedge T_{2i-1}<+\infty\right]\\
\le&\frac{2M_n^2t(t+4)}{\delta^2}.
\end{aligned}$$

By selecting a sufficiently small T satisfying $\frac{2M_n^2T(T+4)}{\delta^2}<\frac{\epsilon}{2}$, we have

$$\begin{aligned}
&\mathbb{P}\left[T_{2i}-T_{2i-1}>T;\ \zeta=+\infty,\ T_{2i-1}<+\infty\right]\\
=&\mathbb{P}\left[\zeta=+\infty,\ T_{2i-1}<+\infty\right]\\
&-\mathbb{P}\left[T_{2i}-T_{2i-1}\le T;\ \zeta=+\infty,\ T_{2i-1}<+\infty\right]\\
\ge&\mathbb{P}\left[\{\zeta=+\infty\}\cap\left\{\limsup_{t\to+\infty}h(\boldsymbol{x}_t)>2\epsilon\right\}\right]\\
&-\mathbb{P}\left[T_{2i}-T_{2i-1}\le T;\ \zeta=+\infty,\ T_{2i-1}<+\infty\right]\ge\frac{\epsilon}{2},
\end{aligned}$$

All these estimations together yield a lower bound for the expectation of the stopping time differences as

$$\begin{aligned}
&\mathbb{E}\left[T_{2i}-T_{2i-1};\ \zeta=+\infty,T_{2i-1}<+\infty\right]\\
&\ge T\mathbb{P}\left[T_{2i}-T_{2i-1}>T;\zeta=+\infty,T_{2i-1}<+\infty\right]\ge\frac{T\epsilon}{2}.
\end{aligned}$$

This, together with (23), results in

$$\begin{aligned}
n\ge&\frac{\epsilon}{2}\sum_{i=1}^{+\infty}\mathbb{E}\left[T_{2i}-T_{2i-1};\ \zeta=+\infty,\ T_{2i-1}<+\infty\right]\\
\ge&\frac{\epsilon}{2}\sum_{i=1}^{+\infty}\frac{T\epsilon}{2}=+\infty.
\end{aligned}$$

This however is a contradiction, which implies a completion of the proof. ∎

References

[1] LaSalle J. Some extensions of Liapunov's second method[J]. IRE Transactions on Circuit Theory, 1960, 7(4): 520-527.
[2] Ryan E P. An integral invariance principle for differential inclusions with applications in adaptive control[J]. SIAM Journal on Control and Optimization, 1998, 36(3): 960-980.
[3] Nolen J. An invariance principle for random traveling waves in one dimension[J]. SIAM journal on mathematical analysis, 2011, 43(1): 153-188.
[4] Hale J K, Lunel S M V. Introduction to functional differential equations[M]. Springer Science & Business Media, 2013.
[5] Slemrod M. Asymptotic behavior of a class of abstract dynamical systems[J]. Journal of Differential Equations, 1970, 7(3): 584-600.
[6] Sell G R. Nonautonomous differential equations and topological dynamics I. The basic theory[J]. Transactions of the American Mathematical Society, 1967, 127(2): 241-262.
[7] Sell G R. Nonautonomous differential equations and topological dynamics. II. Limiting equations[J]. Transactions of the American Mathematical Society, 1967, 127(2): 263-283.
[8] Hespanha J P. Uniform stability of switched linear systems: Extensions of LaSalle's invariance principle[J]. IEEE Transactions on Automatic Control, 2004, 49(4): 470-482.
[9] Bacciotti A, Mazzi L. An invariance principle for nonlinear switched systems[J]. Systems & Control Letters, 2005, 54(11): 1109-1119.
[10] Gammaitoni L, Hänggi P, Jung P, et al. Stochastic resonance[J]. Reviews of Modern Physics, 1998, 70(1): 223.
[11] Appleby J A D, Mao X, Rodkina A. Stabilization and destabilization of nonlinear differential equations by noise[J]. IEEE Transactions on Automatic Control, 2008, 53(3): 683-691.
[12] Ren W, Xiong J. Krasovskii and Razumikhin stability theorems for stochastic switched nonlinear time-delay systems[J]. SIAM Journal on Control and Optimization, 2019, 57(2): 1043-1067.
[13] Li H, Ding X. A control Lyapunov function approach to feedback stabilization of logical control networks[J]. SIAM Journal on Control and optimization, 2019, 57(2): 810-831.
[14] Huang G, Liu X, Takeuchi Y. Lyapunov functions and global stability for age-structured HIV infection model[J]. SIAM Journal on Applied Mathematics, 2012, 72(1): 25-38.
[15] Guo Y, Lin W, Chen G. Stability of switched systems on randomly switching durations with random interaction matrices[J]. IEEE Transactions on Automatic Control, 2017, 63(1): 21-36.
[16] Guo Y, Lin W, Chen Y, et al. Instability in time-delayed switched systems induced by fast and random switching[J]. Journal of Differential Equations, 2017, 263(2): 880-909.
[17] Guo Y, Lin W, Sanjuan M A F. The efficiency of a random and fast switch in complex dynamical systems[J]. New Journal of Physics, 2012, 14(8): 083022.
[18] Guo Y, Lin W, Ho D W C. Discrete-time systems with random switches: From systems stability to networks synchronization[J]. Chaos, 2016, 26(3): 033113.
[19] Khasminskii R. Stochastic stability of differential equations[M]. Springer Science & Business Media, 2011.
[20] Mao X. Stochastic stabilization and destabilization[J]. Systems & Control Letters, 1994, 23(4): 279-290.
[21] Mao X, Yin G G, Yuan C. Stabilization and destabilization of hybrid systems of stochastic differential equations[J]. Automatica, 2007, 43(2): 264-273.
[22] Wu Z, Xia Y, Xie X. Stochastic Barbalat's lemma and its applications[J]. IEEE Transactions on Automatic Control, 2011, 57(6): 1537-1543.
[23] Wu Z, Karimi H R, Shi P. Dissipativity-based small-gain theorems for stochastic network systems[J]. IEEE Transactions on Automatic Control, 2015, 61(8): 2065-2078.
[24] Wen G, Yu W, Hu G, et al. Pinning synchronization of directed networks with switching topologies: A multiple Lyapunov functions approach[J]. IEEE Transactions on Neural Networks and Learning Systems, 2015, 26(12): 3239-3250.
[25] Rodrigues H M, Alberto L F C, Bretas N G. On the invariance principle: Generalizations and applications to synchronization[J]. IEEE Transactions on Circuits and Systems I: Fundamental Theory and Applications, 2000, 47(5): 730-739.
[26] Church K E M, Liu X. Cost-effective robust stabilization and bifurcation suppression[J]. SIAM Journal on Control and Optimization, 2019, 57(3): 2240-2268.
[27] Nijholt E, Rink B, Sanders J. Center manifolds of coupled cell networks[J]. SIAM Journal on Mathematical Analysis, 2017, 49(5): 4117-4148.
[28] Lin W, Chen X, Zhou S. Achieving control and synchronization merely through a stochastically adaptive feedback coupling[J]. Chaos, 2017, 27(7): 073110.
[29] Oksendal, B. Stochastic Differential Equations and Their Applications. World Scientific Press, New York, NY, USA, 2005.
[30] Liptser R, Shiryayev A N. Theory of Martingales[M]. Springer Science & Business Media, 2012.
[31] Mao X. A note on the LaSalle-type theorems for stochastic differential delay equations[J]. Journal of Mathematical Analysis and Applications, 2002, 268(1): 125-142.
[32] Mao X. LaSalle-type theorems for stochastic differential delay equations[J]. Journal of Mathematical Analysis and Applications, 1999, 236(2): 350-369.
[33] Mao X. Stochastic versions of the LaSalle theorem[J]. Journal of Differential Equations, 1999, 153(1): 175-195.
[34] Mao X. Exponential Stability of Stochastic Differential Equations[M]. Marcel Dekker, 1994.
[35] Yuan C, Mao X. Asymptotic stability and boundedness of stochastic differential equations with respect to semimartingales[J]. 2003.
[36] Mao X. Some contributions to stochastic asymptotic stability and boundedness via multiple Lyapunov functions[J]. Journal of Mathematical Analysis and Applications, 2001, 260(2): 325-340.
[37] Shuai Z, van den Driessche P. Global stability of infectious disease models using Lyapunov functions[J]. SIAM Journal on Applied Mathematics, 2013, 73(4): 1513-1532.
[38] Shu H, Wang L, Watmough J. Global stability of a nonlinear viral infection model with infinitely distributed intracellular delays and CTL immune responses[J]. SIAM Journal on Applied Mathematics, 2013, 73(3): 1280-1302.

[39] Lyapunov A M. The general problem of the stability of motion[J]. International Journal of Control, 1992, 55(3): 531-534.
[40] Chow S N, Hale J K. Methods of bifurcation theory[M]. Springer Science & Business Media, 2012.
[41] Karydas N, Schinas J. The center manifold theorem for a discrete system[J]. Applicable Analysis, 1992, 44(3-4): 267-284.
[42] Liptser R S. A strong law of large numbers for local martingales[J]. Stochastics, 1980, 3(1-4): 217-228.
[43] Hu S, Liao X, Mao X. Stochastic Hopfield neural networks[J]. Journal of Physics A: Mathematical and General, 2003, 36(9): 2235.
[44] Cheng C Y, Lin K H, Shih C W. Multistability in recurrent neural networks[J]. SIAM Journal on Applied Mathematics, 2006, 66(4): 1301-1320.
[45] Hespanha J P. Uniform stability of switched linear systems: Extensions of LaSalle's invariance principle[J]. IEEE Transactions on Automatic Control, 2004, 49(4): 470-482.
[46] Mao X, Yin G G, Yuan C. Stabilization and destabilization of hybridsystems of stochastic differential equations[J]. Automatica, 2007, 43(2):264-273
[47] Zong X, Yin G, Li T, et al. Stability of stochastic functional differential systems using degenerate Lyapunov functionals and applications[J]. Automatica, 2018, 91: 197-207.
[48] Yang J, Liu X, Liu X. Stability of stochastic functional differential systems with semi-Markovian switching and Lévy noise by functional Itô's formula and its applications[J]. Journal of the Franklin Institute, 2020, 357(7): 4458-4485.
[49] Zong X, Yin G, Li T, et al. Stability of stochastic functional differential systems using degenerate Lyapunov functionals and applications[J]. Automatica, 2018, 91: 197-207.
[50] Fan L, Zhu Q. pth Moment Exponential Stability of Switched Discrete Time Stochastic Systems: A Multiple Lyapunov Functions Method[J]. Journal of the Franklin Institute, 2021.
[51] Yin J, Khoo S, Man Z, et al. Finite-time stability and instability of stochastic nonlinear systems[J]. Automatica, 2011, 47(12): 2671-2677.
[52] Yu X, Yin J, Khoo S. Generalized Lyapunov criteria on finite-time stability of stochastic nonlinear systems[J]. Automatica, 2019, 107: 183-189.
[53] Teel A R, Subbaraman A, Sferlazza A. Stability analysis for stochastic hybrid systems: A survey[J]. Automatica, 2014, 50(10): 2435-2456.
[54] Berger G O, Jungers R M. p-dominant switched linear systems[J]. Automatica, 2021, 132: 109801.
[55] Ize, Jorge. Topological bifurcation[M]. Topological nonlinear analysis. Birkhäuser Boston, 1995. 341-463.
[56] Khalil H K. Lyapunov stability[J]. Control Systems, Robotics and AutomatioN–Volume XII: Nonlinear, Distributed, and Time Delay Systems-I, 2009: 115.
[57] Shevitz D, Paden B. Lyapunov stability theory of nonsmooth systems[J]. IEEE Transactions on automatic control, 1994, 39(9): 1910-1914.
[58] Aubin J P. Applied functional analysis[M]. John Wiley & Sons, 2011.
[59] Hu S, Liao X, Mao X. Stochastic Hopfield neural networks[J]. Journal of Physics A: Mathematical and General, 2003, 36(9): 2235.
[60] Hu Q, Wu J. Global Hopf bifurcation for differential equations with state-dependent delay[J]. Journal of Differential Equations, 2010, 248(12): 2801-2840.
[61] Wu J, Campbell S A, Bélair J. Time-Delayed Neural Networks: Stability and Oscillations[J]. 2014.
[62] Sirignano J, Spiliopoulos K. Mean field analysis of neural networks: A law of large numbers[J]. SIAM Journal on Applied Mathematics, 2020, 80(2): 725-752.
[63] Nguyen D H, Yin G, Zhu C. Long-term analysis of a stochastic SIRS model with general incidence rates[J]. SIAM Journal on Applied Mathematics, 2020, 80(2): 814-838.
[64] Nguyen D H, Strickler E. A method to deal with the critical case in stochastic population dynamics[J]. SIAM Journal on Applied Mathematics, 2020, 80(3): 1567-1589.